



# Effect of the ball burnishing on the surface quality and mechanical properties of a TRIP steel sheet

Gustavo Capilla-González<sup>1</sup> · Israel Martínez-Ramírez<sup>1</sup> · David Díaz-Infante<sup>2</sup> · Eric Hernández-Rodríguez<sup>1</sup> · Víctor Alcántar-Camarena<sup>3</sup> · Alberto Saldaña-Robles<sup>4</sup>

Received: 2 March 2021 / Accepted: 10 July 2021 / Published online: 24 July 2021  
© The Author(s), under exclusive licence to Springer-Verlag London Ltd., part of Springer Nature 2021

## Abstract

Ball burnishing is a finishing technique involving plastic deformation on the workpiece surface. In this paper, the influence of the ball burnishing operation on the average roughness, tensile properties, anisotropy and work hardening of a TRIP steel was analyzed. An experimental study of the effect of the ball burnishing process on uniaxial tensile specimens was conducted using the Response Surface Methodology (RSM) based on a 3<sup>2</sup> Factorial Design (FD). The effects of burnishing force ( $B_F$ ) and the number of tool passes ( $N_P$ ) on the average roughness ( $R_a$ ), the yield stress ( $\sigma_Y$ ) and the percentage of elongation to fracture (%  $El$ ) were evaluated. The quadratic regression models were obtained to predict  $R_a$  and  $\sigma_Y$  with determination coefficients ( $R^2$ ) of 0.85 and 0.99, respectively. The results indicated that the ball burnishing process produces a maximum reduction of  $R_a$  of 81.7% (from 1.250 to 0.229  $\mu\text{m}$ ). Also, it was observed that the ductility of the material increased in a 25% and the yield stress and work hardening can be substantially modified. Finally, it was found that by using the ball burnishing process, the planar anisotropy of the sheet can be reduced.

**Keywords** Burnishing · Mean roughness · AHSS · Ductility · Response surface methodology

## 1 Introduction

In recent decades, new materials have been used in automotive, aerospace and other manufacturing industries to improve safety, fuel efficiency and manufacturability issues. For instance, Advanced High Strength Steels (AHSS) are widely used for the manufacturing of structural components due to their high strength and energy absorption during impacts. These components manufactured by forming operations are subjected to large deformations under

different stress states. However, springback and reduced formability are typical challenges when forming AHSS [1]. On the one hand, springback phenomenon is related to mechanical properties of the material such as the elastic modulus, the yield stress and ultimate stress [2]. On the other hand, formability could be evaluated by analyzing the plastic flow curve and the deformation process of the material [3]. Also, in sheet metal forming operations where the material is deformed by the action of rigid tools, the friction between the sheet and tools, affecting the strain distribution of the sheet, takes a special role on the fracture of the material [4–9]. Therefore, several authors have focused on the usage of surface plastic deformation techniques, such as the burnishing process, to improve material characteristics like roughness, hardness, fatigue life, microstructure, corrosion resistance and the mechanical properties of materials [10–14]. In recent years, burnishing is considered as one of the outstanding cold-forming finishing processes employed as a surface treatment technique for the manufacturing industry [15]. Burnishing process provides advantages in comparison with other mechanical surface treatments such as shot peening and sand blasting, due to burnishing enhances

✉ Alberto Saldaña-Robles  
alberto.saldana@ugto.mx

<sup>1</sup> Mechanical Engineering Department, University of Guanajuato, 36885, Salamanca, Gto., Mexico

<sup>2</sup> Applied Research, Nidec Minster Corporation, 240 W 5th St, Minster, OH, 45865, USA

<sup>3</sup> Industrial Design Engineering Department, Universidad Politécnica Bicentenario, 36283, Silao, Gto., Mexico

<sup>4</sup> Agricultural Engineering Department, University of Guanajuato, 36500, Irapuato, Gto., México

the smoothness of surfaces (decreases roughness) [16–20], increases the shape and dimensional accuracy [15, 20], induces a higher layer of compressive stress, stronger work-hardened layer [18] and the smoother surfaces produced by burnishing process may be more effective in enhancing the resistance to fatigue crack nucleation in contrast with shot peening [17, 18]. Also, the burnishing process is a low-cost and simple to implement in contrast to other mechanical surface treatments [21].

In the ball burnishing process, the burnishing tool uses a diamond ball to apply a considerable pressure, which leads to microdeformation on the workpiece surface. During this microdeformation, the material is displaced from peaks to valleys of the roughness profile due to elastic-plastic contact mechanism [22, 23]. In the literature, numerous studies have been focused on experimental researches of the ball burnishing process, in order to determine the optimal process parameters for a specific material. Some of the relevant studies are summarized below.

Gharbi et al. [20] evaluated the effect of the ball burnishing parameters on the surface quality and ductility of aluminum 1050A by using uniaxial tensile test specimens. The reported results show that the burnishing process reduced the mean roughness, while the ductility represented by the percentage of elongation increased in 48% in comparison with the unburnished sample. Also, a considerable change in the work hardening of the material was observed [24]. Gharbi et al. [25] investigated the influence of the ball burnishing on the surface quality, ductility and fatigue strength of AISI 1010 steel sheets. The results showed that the optimal burnishing parameters increase the ductility in 49% while the mean roughness was reduced [25]. Similar to Gharbi et al., Khalid and Mayas [26] found that the burnishing process influenced on the ductility of O<sub>1</sub> alloy steel. The results showed that the percentage of elongation increased around 13.6%, while a reduction of 12.5% on the surface quality was observed. Travieso et al. analyzed the effect of the ball burnishing on the low cycle fatigue strength of AISI 1038 steel bars exposed to alternate bending stresses. The authors found that the burnishing process can increase the surface hardness and lifespan of the component by 41% and 77%, respectively [13]. Rodríguez et al. conducted an experimental study of the ball burnishing process on 1045 steel. The results showed that the burnishing process allowed to reduce the surface roughness in 90% and increase the hardness by 60% [27]. Amdouni et al. investigated a new ball burnishing strategy on the flat surface of 2017A-T451 aluminum alloy. As a result, the burnishing process improved the surface roughness and hardness approximately in 81% and 17%, respectively [28]. Hamadache et al. evaluated the work hardening coefficient

and the capacity of the 36 NiCrMo 6 steel to resist surface plastic deformation after the ball burnishing process. They found that the strain hardening coefficient increase around 10% in comparison with the turned surface [29]. Jerez et al. designed a new vibration-assisted ball burnishing (VABB) tool and tested its effectiveness on Ti-6AL-4V flat surfaces. The study revealed that the use of VABB process showed an enhancement in the average roughness of 61.6% and the total roughness of 66.1% [30]. Revankar et al. found that ball burnishing process reduced the surface roughness from 0.45 to 0.12  $\mu\text{m}$ , the friction coefficient was decreased in around 64% and the wear rate was reduced by 52% [14]. Other relevant studies have been demonstrated that the ball burnishing process allows to improve the mechanical and physical properties of the materials. Amini et al. implemented the ultrasonic-assisted ball burnishing process on aluminum 6061 and 1045 steel plates to enhance its surface properties [31]. López et al. used the ball burnishing to improve the final quality of forming tools [32]. Jerez et al. studied the influence of the VABB process on flat surfaces of AISI 1038 alloy, in order to improve the surface quality, wear and fatigue resistance of industrial parts [33]. Franzen et al. analyzed a roller burnishing technique in a thermal sprayed coated DP600 steel. By performing a strip drawing test, concluded that the use of the burnishing parameters influences the tribological conditions [34]. Recently, the effect of the ball burnishing process has taken a great interest due to the wide use of these materials in automotive components. To mention, Travieso et al. analyzed the effect of the plastic deformation generated by the ball burnishing process on several types TRIP sheets with different content of martensite [35].

The reviewed literature exhibits the benefits of the ball burnishing process on the surface integrity of the materials, especially for mild steels and aluminum alloys. Some studies show that the burnishing force is the most influential burnishing parameter on the surface integrity of diverse materials [36–38]. However, there is a lack of information regarding the influence of the ball burnishing process in materials with unique properties such as the AHSS steels. The present work aims to present the influence of the ball burnishing force and the number of tool passes on the surface quality of a TRIP steel sheet by analyzing the mean surface roughness. Also, by uniaxial tensile tests, the experimentally determined stress-strain curves were processed to analyze the tensile properties, anisotropy and work hardening for the burnishing conditions. The results presented in this work will provide important information for the study and application of the ball burnishing process in automotive components where the strength, ductility, fatigue life and surface finishing are of main importance.

## 2 Experimental procedures

### 2.1 Material preparation

Transformation Induced Plasticity (TRIP) steel, 1.1 mm thick, was used in the experiments. TRIP steel is a low alloy multiphase steel that combines high strength and good formability due to its microstructure of retained austenite embedded in a primary matrix of ferrite. The chemical composition of the used material is listed in Table 1.

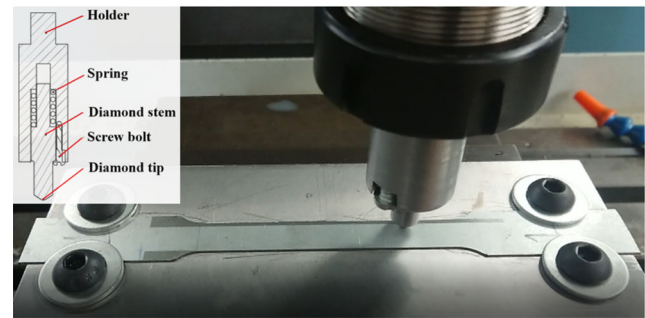
From the received material, the uniaxial tensile test specimens according to the ASTM E-8 [39] standard were cut by laser in three angles from the rolling direction of the sheets (i.e., 0°, 45° and 90°). Once cut, specimens were deburred to eliminate sharp edges produced during the cutting process. Extensometer lines and initial cross section dimensions were measured to calculate the stress-strain response of the sheet.

### 2.2 Burnishing procedure

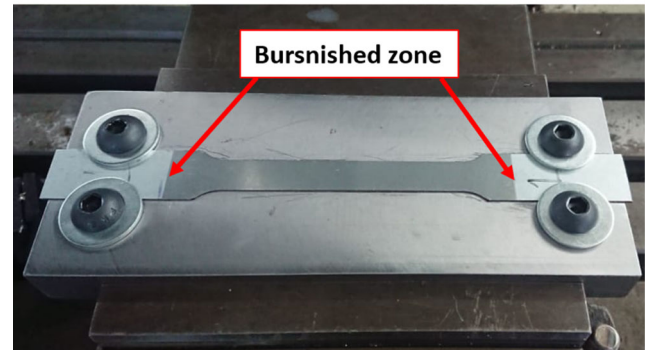
A rectangular mold with the specimen geometry was machined with a parallel deviation less than 0.01 mm. The mold was fixed on the bed of a machining center VIWA model VCM1050M400-T. The diamond stem was mounted in a specially designed holder attached in a 25-mm ER40 collet chuck. In this work, in order to evaluate the influence of the burnishing force  $B_F$  and the number of tool passes  $N_P$ , five burnishing forces  $B_F = 50\text{ N}$ , 150 N, 250 N, 300 N and 500 N with  $N_P = 1, 2, 3$  were considered in the experimental study. The front and back faces of the specimens were burnished using a travel speed of 2000 mm/min. The burnishing process and a burnished specimen are presented in Fig. 1(a) and (b), respectively.

Before the burnishing operation, a calibration curve was obtained to correlate the vertical displacement of the diamond stem with the applied vertical force. The force was measured by an Extech digital force gauge and the vertical displacement was obtained from the machining center. Thus, the application of the predefined burnishing forces in this study was controlled by the vertical displacement of the machining center.

For the burnishing process, a toolpath parallel to the tensile direction of the sheet with a stepover  $S_0 = 50\%$  of the diamond tip trace was considered (see Fig. 2). In order to preserve an homogeneous strain state in the specimen, the burnished zone was considered up to 10 mm of the gripping



(a)



(b)

**Fig. 1** Experimental setup of the ball burnishing process: (a) burnishing tool, (b) burnished specimen

area of the specimens. Previous experiments performed by the present authors showed that when the burnishing is conducted just on the gauge length of the specimen, in most of the cases the fracture will take place out of this region.

To evaluate the stepover distance, the diamond tip trace was measured and photographed with a Moticam camera attached to a tool's maker microscope. To mention, the photographs of the diamond tip trace for the burnishing forces  $B_F = 50\text{ N}$  and  $B_F = 500\text{ N}$  with a trace width of 0.344 mm and 0.832 mm, respectively are shown in Fig. 3(a)–(b).

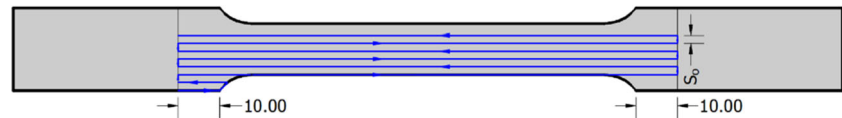
### 2.3 Surface roughness

A surface roughness tester Mitutoyo® model surfstest SJ-310 was employed to measure the surface average roughness  $R_a$  of the unburnished and burnished samples according to the ISO 4287 standard. The measurements were performed using a cutoff length, evaluation length

**Table 1** Chemical composition of the TRIP steel sheet (in % wt)

	C	Si	Mn	P	Al	B	Cr	Cu	Mo	Nb
TRIP	0.22	0.102	1.62	0.013	1.43	0.0002	0.028	0.015	0.003	0.001

**Fig. 2** Toolpath over the calibrated area



and measure speed of 0.8 mm, 4.8 mm and 0.5 mm s<sup>-1</sup>, respectively [40]. The  $R_a$  is determined as the integral of the absolute value of the surface roughness profile height  $|y(x)|$  over the evaluation length ( $l$ ), as shown in Eq. (1) [41]. An average of six measurements of  $R_a$  was determined per each sample with three readings at different points for each burnished side of the sample.

$$R_a = \frac{1}{l} \int_0^l |y(x)| dx \quad (1)$$

## 2.4 Uniaxial tensile test

Uniaxial tensile tests were conducted in an Instron universal testing machine with 25 kN capacity using a crosshead speed of 5 mm/min. The tests were conducted under displacement control up to the fracture of the specimen. To calculate the strain, a 50-mm gauge length extensometer was used. The repeatability of the experiments was confirmed by testing three samples for each condition. After the test, the yield stress  $\sigma_Y$ , ultimate stress  $\sigma_U$ , uniform elongation  $\varepsilon_U$  and percentage of elongation to fracture  $E1\%$  were determined from the engineering stress vs. engineering strain curves. To calculate the yield stress  $\sigma_Y$ , the offset yield stress method at 0.2% of strain from the origin was used. To analyze the work hardening of the material, the fitting of the true stress vs. true strain curves by using the power law model is presented. Finally, to evaluate the influence of the burnishing process on the planar anisotropy, the Lankford coefficients ( $r_0$ ,  $r_{45}$  and  $r_{90}$ ) are calculated at a plastic strain level  $\varepsilon^p = 0.1$  for the reference specimen and those with the higher burnishing force  $B_F = 250$  N with  $N_p = 1, 2$  and 3.

## 2.5 Experimental design and data analysis

A 3<sup>2</sup> Factorial Design (FD) combined with response surface methodology (RSM) was applied to investigate the influence of two burnishing factors on the average surface

roughness and tensile properties in specimens cut at 0° from the rolling direction of the steel sheet. A total of 27 experiments were conducted through the FD, using 3 levels and 2 factors (9 experimental points), which were carried out for triplicate and randomness. Table 2 list the ball burnishing factors and their experimental levels. The Design Expert Software was employed for the statistical design of experiments and data analysis. Also, in order to evaluate  $R_a$  at higher forces, two specimens were burnished using 300 N and 500 N of burnishing force with  $N_p = 2$ , each one for duplicate.

## 3 Results and discussion

### 3.1 Effect of ball burnishing parameters on average surface roughness

The result of the analysis of variance (ANOVA) for the mean surface roughness at 95% of confidence level is presented in Table 3. The  $p$ -values less than 0.05 indicate that the model terms are significant and  $p$ -values less than 0.0001 shows statistically strong significance. It can be observed that both factors, burnishing force ( $B_F$ ) and the number of passes ( $N_p$ ) have a significative effect on  $R_a$  with a percentage contribution of 58.8% and 20.0%, respectively. The regression analysis suggests that the quadratic model presented in Eq. (2) satisfactorily represents  $R_a$  in terms of the factors  $B_F$  and  $N_p$ . The coefficient of determination, denoted by  $R^2$ , provides the ratio of the total variation in the response calculated by the model, indicating the proportion of sum of squares due to regression to total sum of squares [42]. The  $R^2$  value for  $R_a$  model is 0.845; this indicates that the ball burnishing parameters are able to represent 84.5% of the variance in  $R_a$ .

$$R_a = 1.0027 - 3.3510E^{-3} \cdot B_F - 0.3394 \cdot N_p + 3.9600E^{-4} \cdot B_F \cdot N_p + 5.2167E^{-6} \cdot B_F^2 + 0.0573N_p^2 \quad (2)$$

**Fig. 3** Diamond stem trace for (a) 50 N and (b) 500 N

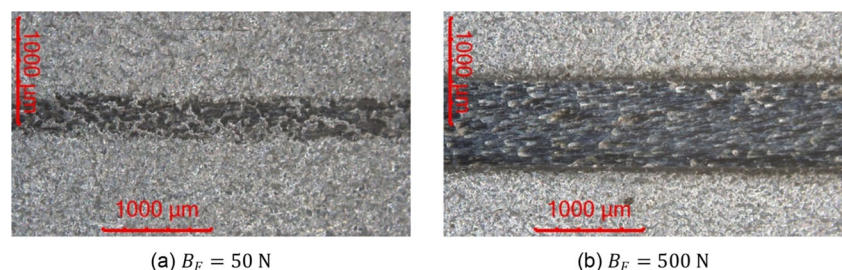


**Table 2** Experimental levels of the ball burnishing factors

Ball burnishing factors	Notation	Code	Levels			
			-1	0	1	
Burnishing force	(N)	$B_F$	A	50	150	250
Number of tool passes	—	$N_P$	B	1	2	3

Figure 4 presents the response surface and contour plot for  $R_a$  as function of the burnishing force and the number of tool passes. It can be observed that the increase in the burnishing force produces a decrease in  $R_a$  in all the burnished specimens with respect to the reference specimen. The initial  $R_a$  of the unburnished specimen was  $1.250\ \mu\text{m}$ , while the minimum and maximum  $R_a$  after ball burnishing were obtained for the burnished condition  $B_F = 250\ \text{N}$  and  $N_P = 2$  and  $B_F = 50\ \text{N}$  and  $N_P = 1$  with  $0.229\ \mu\text{m}$  and  $0.583\ \mu\text{m}$ , respectively. Therefore, the ball burnishing process used in this work allowed to reduce the surface roughness considerably between  $53.4\% \leq R_a \leq 81.7\%$ . It is important to note that although the burnishing condition  $B_F = 250\ \text{N}$  and  $N_P = 2$  has the lowest  $R_a$  ( $0.229\ \mu\text{m}$ ), the burnished condition  $B_F = 150\ \text{N}$  and  $N_P = 1$  also show a low  $R_a$  ( $0.390\ \mu\text{m}$ ) in comparison with the unburnished specimen. This last condition not only allows to obtain an adequate  $R_a$ , but also reduces the burnishing process time in around 50.0%.

The roughness profiles of the unburnished specimen and burnished specimen with  $B_F = 250\ \text{N}$  and  $300\ \text{N}$  for  $N_P = 2$  are shown in Fig. 5. It can be observed that using a  $B_F = 250\ \text{N}$  a smooth roughness profile with  $R_a = 0.243\ \mu\text{m}$  is obtained. Also, this figure shows that although  $R_a$  for the burnished specimen with  $300\ \text{N}$  ( $0.494\ \mu\text{m}$ ) was less than the unburnished specimen ( $1.250\ \mu\text{m}$ ), a pattern on the roughness profile is observed. This is because that for this material and burnishing conditions, it seems to be a threshold force around  $250\ \text{N}$  that when is exceeded, the roughness starts to increase. These high forces can promote

**Table 3** ANOVA results for  $R_a$

Source	SS	DF	MS	F-value	p-value
A- $B_F$	0.1778	1	0.1778	72.86	< 0.0001
B- $N_P$	0.0462	1	0.0462	18.94	0.0003
AB	0.0188	1	0.0188	7.70	0.0113
A <sup>2</sup>	0.0163	1	0.0163	6.69	0.0172
B <sup>2</sup>	0.0197	1	0.0197	8.08	0.0097
Residual	0.0512	21	0.0024		
Total	0.3300	26			

SS sum of squares, DF degree of freedom, MS mean square

excessive plastic deformation and accumulation or stacking of material. According Jerez-Mesa et al. the ball burnishing on TRIP steel produces a surface nanolayer with a thickness of  $100\ \text{nm}$  composed by new nano-grains, probably formed by the recrystallization of the highly deformed surface [35]. Therefore, the roughness profile of the specimen burnished with  $300\ \text{N}$  shows a higher period and amplitude in comparison with the sample burnished with  $250\ \text{N}$ . Also, the result of  $R_a$  for the burnishing force of  $500\ \text{N}$  with  $N_P = 2$  was  $0.524\ \mu\text{m}$ . This suggests that more severe plastic deformation is generated in comparison with the force of  $300\ \text{N}$  ( $0.451\ \mu\text{m}$ ).

### 3.2 Effect of ball burnishing parameters on tensile properties, anisotropy and work hardening

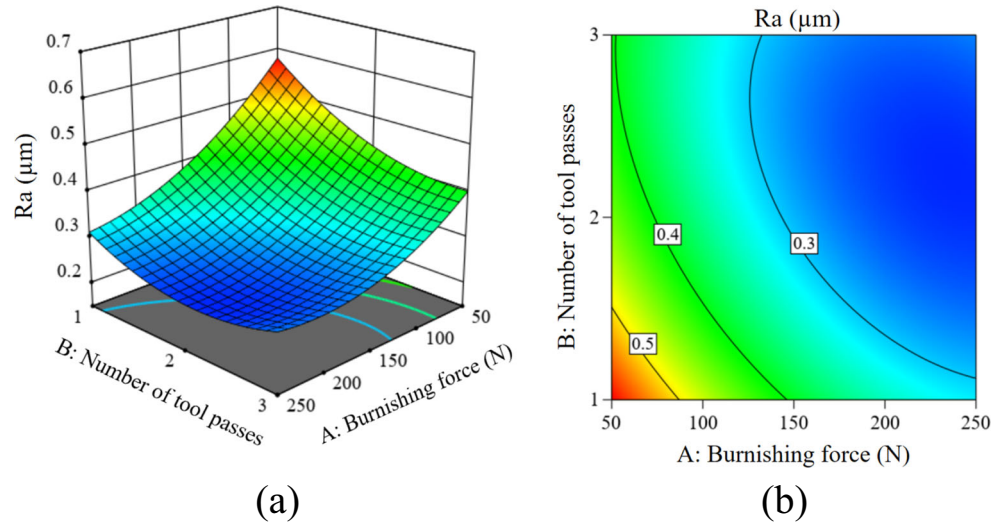
The influence of the ball burnishing process on the yield stress  $\sigma_Y$ , ultimate stress  $\sigma_U$ , uniform elongation  $\epsilon_U$ , percentage of elongation to fracture %  $El$  and the work hardening based on the stress-strain curves of the material were analyzed. These tensile properties are of great interest in sheet metal forming operations when severe plastic deformation, springback and formability are analyzed [2, 43–45].

Table 4 shows the ANOVA result for the yield stress  $\sigma_Y$ . It was found that the burnishing force has a significant effect on the change of  $\sigma_Y$  with a 95% of confidence level. The number of passes  $N_P$  has a low contribution of 6.9%, while the burnishing force has a high percentage contribution of 91.7%. The  $R^2$  value determined for the  $\sigma_Y$  model was 0.99. The relationship between the burnishing factors (burnishing force and number of passes) and the yield stress is shown in Eq. (3).

$$\sigma_y = 401.5 + 7.667E^{-2} \cdot F_B + 29.028 \cdot N_p + 1.500E^{-2} \cdot F_B \cdot N_p + 1.467E^{-3} \cdot F_B^2 - 3.333N_p^2 \quad (3)$$

The effect of burnishing force and the number of passes on the yield stress is shown in Fig. 6(a) and (b). From the response surface shown in Fig. 6(a), it can be observed that an increment of the burnishing force produces a significative increase of the yield stress. However, the number of passes has not so strong influence. The yield stress of the

**Fig. 4** Effect of burnishing force and number of tool passes on  $R_a$ : (a) response surface plot and (b) contour plot



unburnished specimen taken as a reference from the as-received sheet was  $\sigma_Y = 440$  MPa. It can be observed that no significant change on the yield stress  $\sigma_Y$  occurs with the burnishing condition of  $B_F = 50$  N and  $N_p = 1$ . On the other hand, the maximum value of the yield stress was 558 MPa with  $B_F = 250$  N and  $N_p = 3$ . Thus, the ball burnishing process parameters used in this study increase the yield stress around 25.7%. Figure 6(b) shows the contour plot of the yield stress, the burnishing force and number of passes.

Thus, depending on the application, ball burnishing parameters can be selected in order to modify the yield stress of the material; specifically for sheet metal forming operations where this material is highly used. Keeping low values of yield stress will contribute to not increase the springback of the component. In this work, this is obtained with a  $B_F = 50$  N and  $N_p = 1, 2$  or 3, representing a 3.9% of increment in reference with the unburnished specimen. On the other hand, the yield stress of the material can be considerably increased for applications where high strength and energy absorption during impact are required; as is

the case of structural components. In this sense, Fig. 7 shows the effect of the burnishing force with  $N_p = 2$ . For analysis purpose, additional burnishing forces of 300 N and 500 N were included in the study. In this figure, it can be seen that an increase of the ball burnishing force above 250 N continues to increase  $\sigma_Y$ , up to a maximum value of 631 MPa with  $B_F = 500$  N, which is 42.0% higher respect to the reference value. The repeatability of the process is validated by the error bars calculated using the standard deviation shown in Fig. 7.

To analyze the influence of the burnishing parameters  $B_F$  and  $N_p$  on the work hardening and uniform elongation  $\epsilon_U$  of the material, the experimental engineering stress vs. engineering strain curves are shown in Fig. 8(a)–(d). First, it is observed that the burnishing force  $B_F$  has the strongest influence on the work hardening behavior of the sheet, while the number of passes not so. From Fig. 8(a), it is clear that for small burnishing forces (i.e.,  $B_F = 50$  N and 150 N) the stress-strain curve has the same work hardening of the unburnished specimen. However, using a  $B_F = 250$  N, a sharp transition from the elastic to plastic region with higher

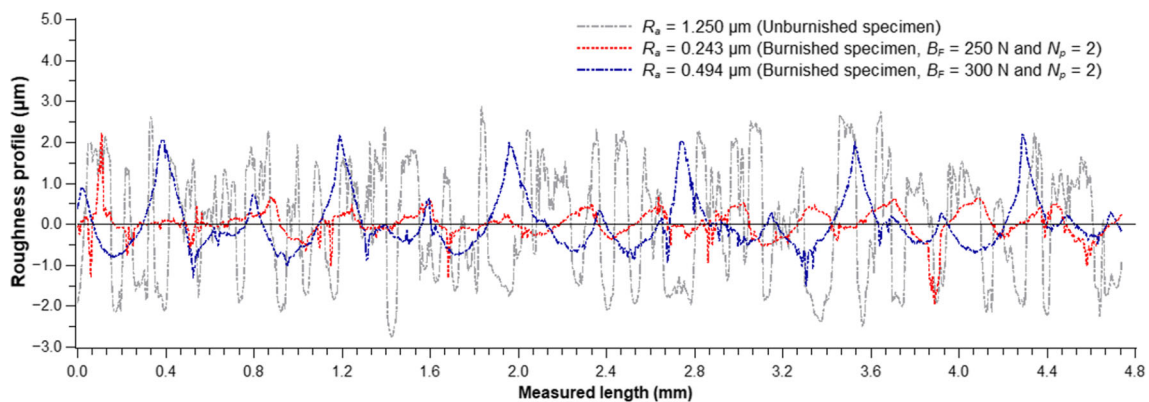


**Fig. 5** Roughness profiles for the unburnished and two burnished specimens

**Table 4** ANOVA result for yield stress  $\sigma_Y$

Source	SS	DF	MS	F-value	p-value
A- $B_F$	42632.00	1	42632.00	1442.18	< 0.0001
B- $N_P$	3253.56	1	3253.56	110.06	< 0.0001
AB	27.00	1	27.00	0.9134	0.3501
A <sup>2</sup>	1290.67	1	1290.67	43.66	< 0.0001
B <sup>2</sup>	66.67	1	66.67	2.26	0.1481
Residual	620.78	21	29.56		
Total	47890.67	26			

yield stress is observed. Similar behavior on the yield stress is observed for the  $N_P = 2$  (see Fig. 8(b)). However, with the same burnishing force but with  $N_P = 3$  (see Fig. 8(c)) a higher work hardening of the stress-strain curve is observed. Additionally, the stress-strain curves using the  $B_F = 300$  N and 500 N, both with  $N_P = 2$ , are presented in Fig. 8(d). Here, a sharper transition from the elastic to plastic region with a well-defined yield point and a clear yield plateau can be observed. This could be attributed to the severe plastic deformation that causes a change in the microstructure of the material. On the other hand, it was found that the uniform elongation  $\epsilon_U$  and the ultimate tensile stress  $\sigma_U$  are not strongly influenced by the burnishing parameters used in this work. These characteristics of the stress-strain curve would provide higher strength to the material without compromise its ductility.

The percentage of elongation to fracture which is an indicator of the ductility of the material is analyzed in Fig. 9. First, from the unburnished specimen a  $\% El = 25.4\%$  was obtained. Also, it can be observed that using a low burnishing force  $B_F = 50$  N the  $\% El$  is increased to a maximum value of 32.4% with  $N_P = 3$ . As is observed,

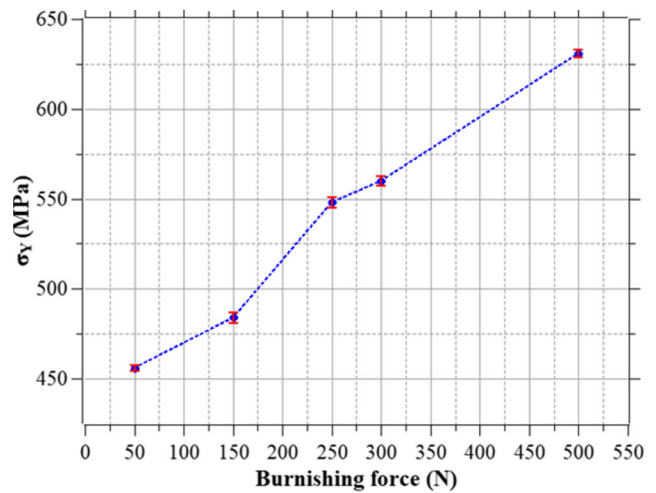
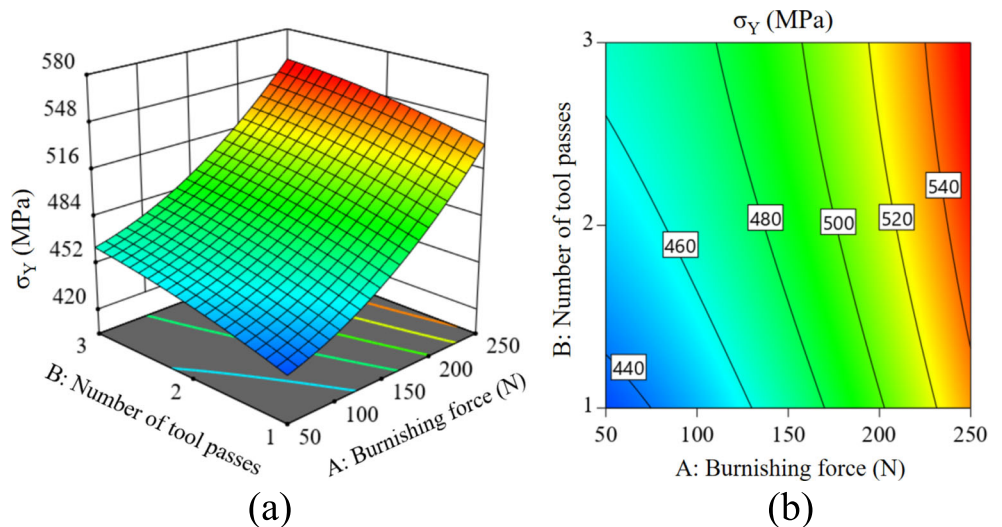


**Fig. 7** Effect of burnishing force on the yield stress  $\sigma_Y$  using  $N_P = 2$

the number of passes has not significant effect for the burnishing forces of 50 N and 150 N. However, when the burnishing force is increased to 250 N, the  $\% El$  decrease to 31% with  $N_P = 2$  and 3, exhibiting higher variability. From the ANOVA results, it was found that the levels of both factors, burnishing force and the number of tool passes are not significant for the percentage of elongation to fracture ( $\% El$ ). However, the factors have strong influence on the  $\% El$ , increasing its value with respect to reference specimen (see Fig. 9).

On the other hand, the planar anisotropy is highly important in sheet metal forming operations as is the deep drawing, where the excessive thinning or earing on the component takes place [46]. The influence of the burnishing process on the planar anisotropy of the sheet in three angles from the rolling direction i.e., 0°, 45° and 90° are presented

**Fig. 6** Effect of burnishing force and number of tool passes on  $\sigma_Y$ : (a) response surface and (b) contour plot



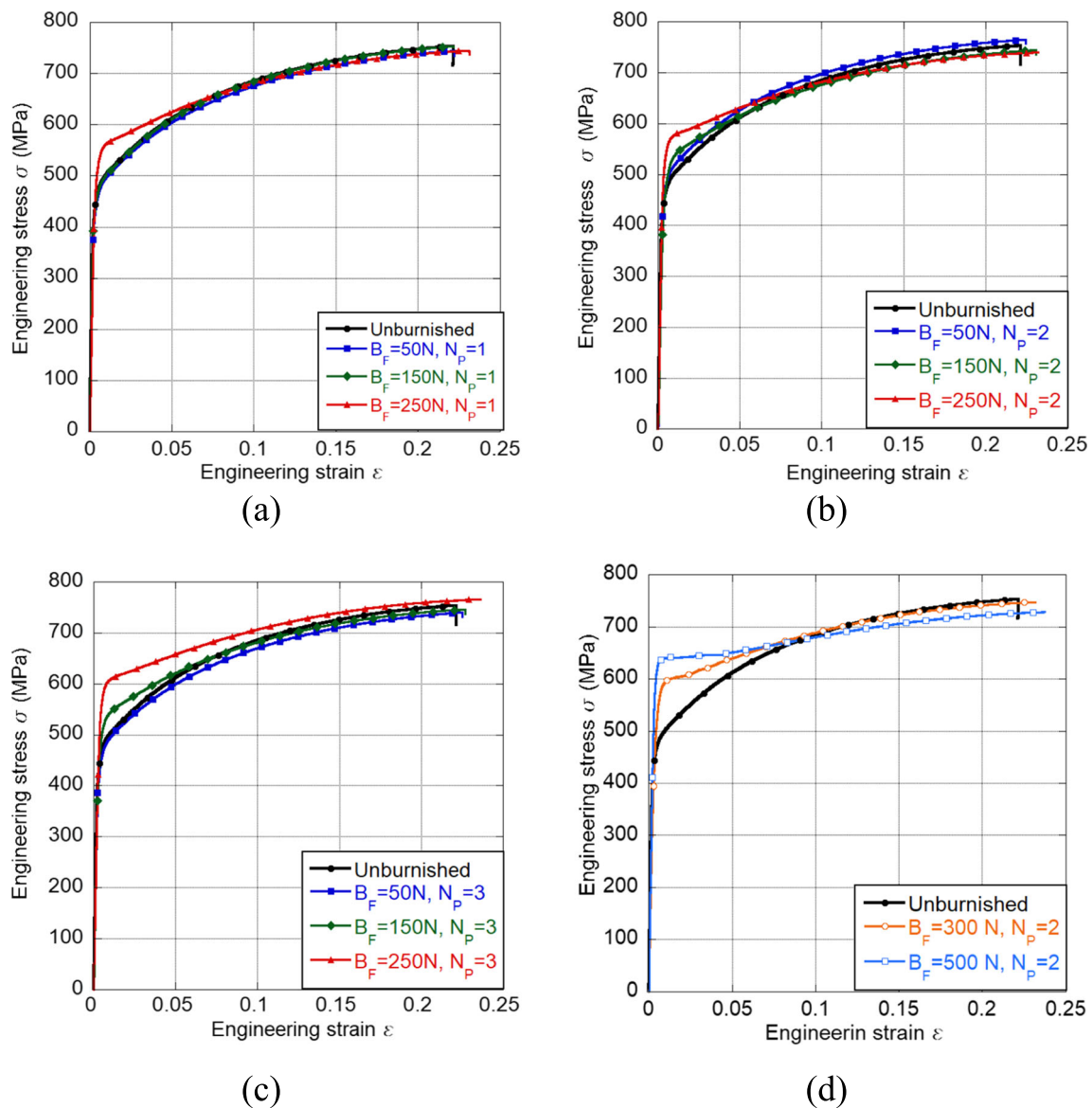


**Fig. 8** Engineering stress vs. engineering strain curves with different ball burnishing conditions: (a) variable  $B_F$  and  $N_p = 1$ , (b) variable  $B_F$  and  $N_p = 2$ , (c) variable  $B_F$  and  $N_p = 3$  and (d)  $B_F = 300$  and  $500$  N and  $N_p = 2$

in Fig. 10. The anisotropy is expressed in terms of the Lankford coefficients  $r_0$ ,  $r_{45}$  and  $r_{90}$ . It can be observed that the as-received sheet (unburnished) exhibit some level of planar anisotropy with values lower than 1.0, in  $0^\circ$  and  $45^\circ$ . On the other hand, it is noted that with the ball burnishing process, the planar anisotropy of the sheet is considerably reduced with values close to 1.0 in all the angles from rolling direction (i.e.,  $1.02 \leq 0^\circ \leq 1.08$ ,  $0.90 \leq 45^\circ \leq 0.93$  and  $0.83 \leq 90^\circ \leq 0.90$ ). Also it can be observed that the number of passes has not strong influence of the material response. This behavior on the anisotropy can be attributed to the plastic deformation on the grains in the

compression layer of the sheet. However, a deep study on the microstructural change will be useful to fully understand the evolution of the anisotropy with the burnishing process in different materials.

The strain hardening exponent  $n$  (or  $n$ -value) plays a crucial role in sheet metal forming. Typically, materials that exhibit higher  $n$ -values have better formability than those with low  $n$ -values. The hardening exponent was determined by assuming the power law ( $\sigma = K \epsilon^n$ ) for the description of the true stress vs. true strain curves. On the logarithmic scale, the linear hardening exponent was calculated at plastic strain level between  $0.1 \leq \epsilon^p \leq 0.2$ .



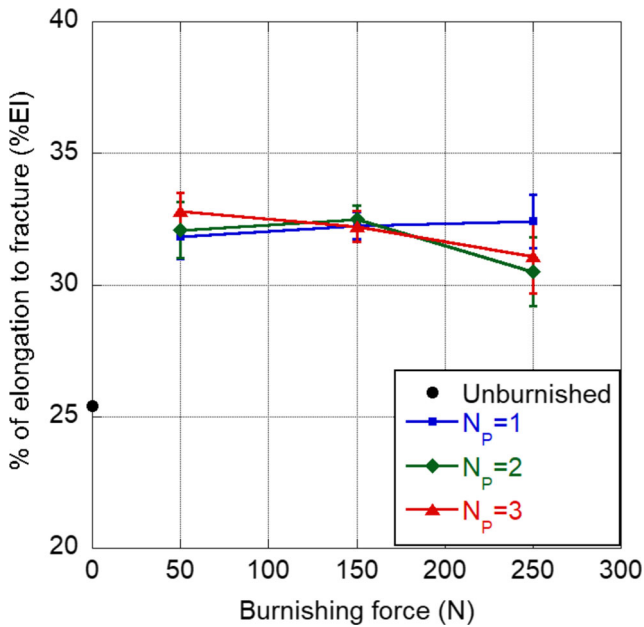
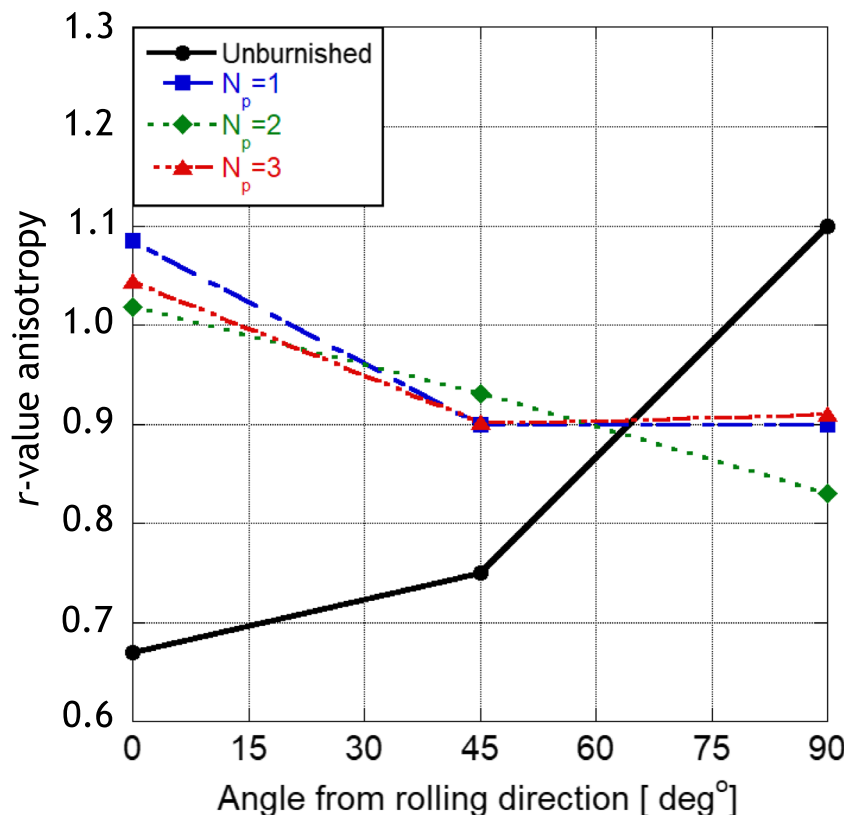


Fig. 9 Effect of the burnishing force on the % of elongation to fracture for different number of passes

Figure 11 shows the hardening exponent results of the unburnished specimen and those obtained with  $B_F = 50, 150$  and  $250$  N with  $N_p = 1, 2$  and  $3$ . It can be observed that by using a low burnishing force ( $B_F = 50$ ), the  $n$ -

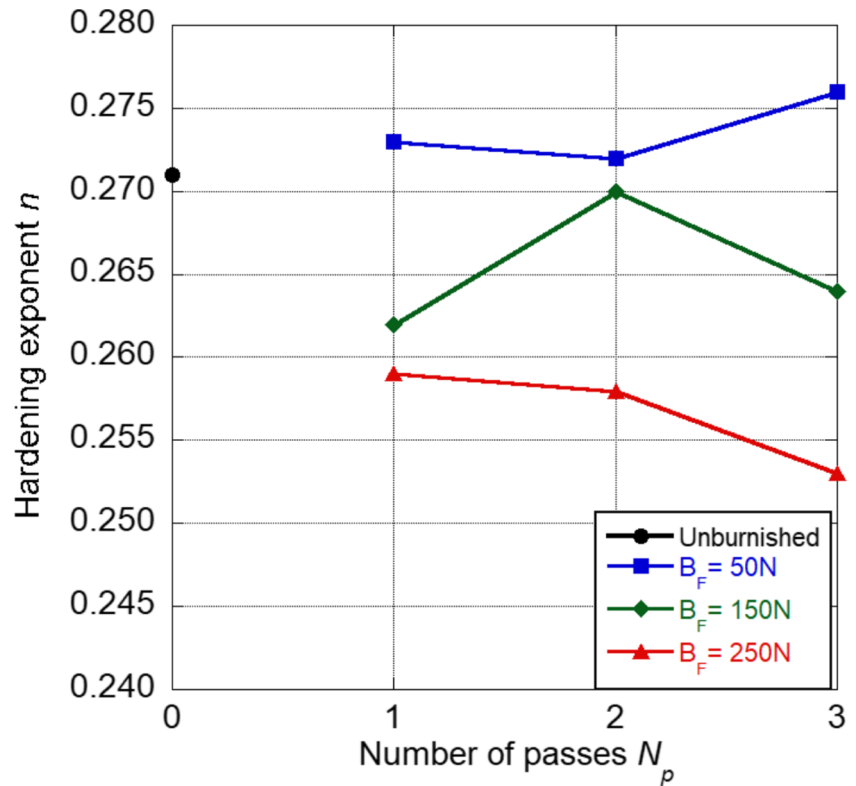
Fig. 10 Influence of the burnishing process in the anisotropy by using a  $B_F = 250$  N with different numbers of passes



value slightly increased in reference with the unburnished specimen, especially with  $N_p = 3$ . On the other hand, with the burnishing forces  $B_F = 150$  and  $250$  N, the hardening exponent was slightly reduced. This suggests that with the appropriate ball burnishing parameters, the formability of the sheets (increase of the  $n$ -value) can be enhanced. To represent the work hardening of the sheet, the true stress vs. true strain curves determined from the experiment and the fitting with the power law hardening model for a  $B_F = 50, 150$  and  $250$  N with  $N_p = 3$  are shown in Fig. 12.

As shown by the experimental results, the surface finish of the TRIP steel is improved by the ball burnishing. The roughness can be decreased by increasing the burnishing force for any value of the number of passes. In this sense, Fargas et al. reported the formation of a surface layer on metastable austenitic steels subjected to plastic deformation by a plastic deformation process. They showed that this surface layer suffered a phase transformation (from austenite to martensite) after the surface deformation. In this case, the phase transformation improved the hardness and fatigue limit of samples [47]. Silva-Álvarez et al. reported that ball burnishing produces a compressive residual stress on the surface of a metallic substrate [48]. In our case, the ball burnishing produced an increase on the yield stress (see Fig. 7) which could be explained in terms of the surface transformations due to the plastic deformation produced by the surface treatment, as found in the researches described

**Fig. 11** Influence of the burnishing process on the hardening exponent  $n$



above. The presence of the compressive residual stress and the new surface layer improve the resistance to crack initiation and propagation. In future works, microstructural and residual stress analysis could be implemented to investigate the influence of the ball burnishing process on this material.

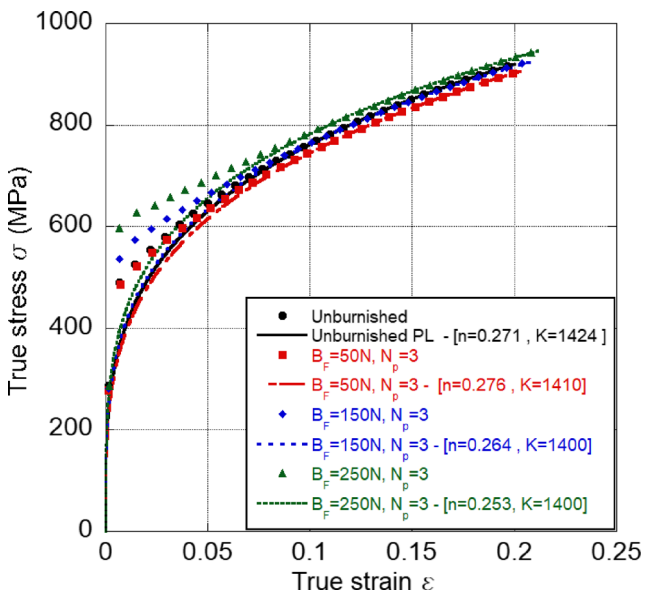


**Fig. 12** Fitting of the stress-strain curves by using the power law

### 4 Conclusions

The experimental results presented in this work show the effects of the ball burnishing force and number of tool passes on the surface mean roughness, tensile properties, anisotropy and work hardening of a TRIP steel sheet. The ANOVA results proved that the burnishing force has a significant effect on roughness and yield stress with contributions of 58.8% and 91.7%, respectively. It was found that the ball burnishing process with  $B_F = 250 N$  and  $N_p = 2$  passes exhibit excellent results in mean roughness, ductility and tensile properties. On the one hand, this ball burnishing condition allowed to reduce  $R_a$  considerably from 1.250 to 0.229  $\mu m$ , representing a reduction of 81.7% in the surface mean roughness. Also, the % elongation to fracture (%  $El$ ) was enhanced from 25.4 to 32.4%. Regarding the tensile properties, yield stress goes from 444.0 to 631 MPa, representing a 42% of increment. Also, it was observed that the hardening exponent related with the formability of the sheet can be increased if the adequate burnishing force is used. Finally it was found that the anisotropy of the sheet is minimized with the burnishing process exhibiting values closer to the unity (isotropic). Thus, the application of the ball burnishing process on these types of materials can be used to improve the surface quality, ductility and strength of the material; especially for sheet metal forming applications where large deformations are expected, as well as to enhance the energy absorption

during impacts. In future works, complementary techniques to analyze the microstructural change and residual stress are necessary to increase the understanding of the ball burnishing influence on this type of advanced materials.

**Author contribution** All authors certify that they have participated sufficiently in the work to take public responsibility for the content, including participation in the concept, design, analysis, writing, or revision of the manuscript.

**Funding** No funding was received to assist with the preparation of this manuscript.

**Availability of data and materials** The authors confirm that the data supporting the findings of this study are available within the article.

## Declarations

**Ethics approval** Each author certifies that this material or similar material has not been and will not be submitted to or published in any other publication before its appearance in *The International Journal of Advanced Manufacturing Technology*.

**Consent to participate** All authors agree to participate in the research study understanding the purpose and nature of this study and participating voluntarily.

**Consent for publication** All authors have participated in approval of the final version for the publication of this paper.

**Conflict of interest** The authors declare no competing interests.

## References

1. Takahashi M et al (2003) Development of high strength steels for automobiles. *Shinnittetsu Giho*, pp 2–6
2. Kim H, Kimchi M, Altan T (2009) Control of springback in bending and flanging advanced high strength steels (ahss). In: International automotive body congress (IABC). Citeseer, Troy, Michigan, USA, p 2009
3. Butuc MC, Teodosiu C, Barlat F, Gracio JJ (2011) Analysis of sheet metal formability through isotropic and kinematic hardening models. *Eur J Mech -A/Solids* 30(4):532–546
4. Lee J-Y, Barlat F, Lee M-G (2015) Constitutive and friction modeling for accurate springback analysis of advanced high strength steel sheets. *Int J Plast* 71:113–135
5. Zhang Z, Lee D (1995) Effect of process variables and material properties on the springback behavior of 2d-draw bending parts. SAE Technical Paper, Tech. Rep.
6. Albut A (2006) Influence of the friction coefficient on springback effect of a u-shaped part manufactured by tailor welded stripes. *Univ Politehnica Bucharest Sci Bull Ser D Mech Eng* 68(3):27–36
7. Trzepieciński T (2020) Effect of the plastic strain and drawing quality on the frictional resistance of steel sheets. *Acta Metall Slovaca* 26:42–44
8. Evin E, Tomáš M, Kollárová M, Antoszewski B (2014) Some tribological aspects of fe-zn coated steel sheets at stamping processes. *Acta Metall Slovaca* 20(2):189–199
9. Wang W, Zhao Y, Wang Z, Hua M, Wei X (2016) A study on variable friction model in sheet metal forming with advanced high strength steels. *Tribol Int* 93:17–28
10. Jerez-Mesa R, Fargas G, Roa J, Llumà J, Travieso-Rodríguez J (2021) Superficial effects of ball burnishing on trip steel AISI 301LN, sheets. *Metals* 2021 11:82
11. Llumà J, Gómez-Gras G, Jerez-Mesa R, Rue-Mascarell J, Travieso-Rodríguez JA (2020) Mechanical strengthening in s235jr steel sheets through vibration-assisted ball burnishing. *Metals* 10(8):1010
12. Chomienne V, Valiorgue F, Rech J, Verdu C (2016) Influence of ball burnishing on residual stress profile of a 15-5ph stainless steel. *CIRP J Manuf Sci Technol* 13:90–96
13. Travieso-Rodríguez JA, Jerez-Mesa R, Gómez-Gras G, Llumà-Fuentes J, Casadesús-Farràs O, Madueño-Guerrero M (2019) Hardening effect and fatigue behavior enhancement through ball burnishing on AISI 1038. *J Mater Res Technol* 8(6):5639–5646
14. Revankar GD, Shetty R, Rao SS, Gaitonde VN (2017) Wear resistance enhancement of titanium alloy (ti-6al-4v) by ball burnishing process. *J Mater Res Technol* 6(1):13–32
15. Shivalingappa D et al (2020) The influence of ball and roller burnishing process parameters on surface integrity of al 2024 alloy. *Mater Today Proc* 27:1337–1340
16. Hassan AM, Momani AM (2000) Further improvements in some properties of shot peened components using the burnishing process. *Int J Mach Tools Manuf* 40(12):1775–1786
17. Mhaede M, Sano Y, Altenberger I, Wagner L (2011) Fatigue performance of Al7075-T73 and Ti-6Al-4V: comparing results after shot peening, laser shock peening and ball-burnishing. *Int J Struct Int* 2(2):185–199
18. Zhang P, Lindemann J (2005) Effect of roller burnishing on the high cycle fatigue performance of the high-strength wrought magnesium alloy AZ80. *Scr Mater* 52(10):1011–1015
19. Ibrahim A, Khalil T, Tawfeek T (2015) Study the influence of a new ball burnishing technique on the surface roughness of AISI 1018 low carbon steel. *Int J Eng Technol* 4(1):227
20. Gharbi F, Sghaier S, Al-Fadhalah K, Benameur T (2011) Effect of ball burnishing process on the surface quality and microstructure properties of AISI 1010 steel plates. *J Mater Eng Perform* 20(6):903–910
21. Sadeler R, Akbulut M, Atasoy S (2013) Influence of mechanical (ball burnishing) surface treatment on fatigue behaviour of AISI 1045 steel. *Kov Mater* 51(1):31–5
22. Shiou F-J, Banh Q-N (2016) Development of an innovative small ball-burnishing tool embedded with a load cell. *Int J Adv Manuf Technol* 87(1):31–41
23. Amini C, Jerez-Mesa R, Travieso-Rodríguez JA, Llumà J, Estevez-Urra A (2020) Finite element analysis of ball burnishing on ball-end milled surfaces considering their original topology and residual stress. *Metals* 10(5):638
24. Gharbi F, Sghaier S, Benameur T (2011) Effect of burnishing parameters on surface quality and ductility of Aluminum 1050A rolled sheet by a newly designed ball burnishing tool, 4th Congrès International Conception et Modélisation des Systèmes Mécaniques CMSM, pp 1–8
25. Gharbi F, Sghaier S, Morel F, Benameur T (2015) Experimental investigation of the effect of burnishing force on service properties of AISI 1010 steel plates. *J Mater Eng Perform* 24(2):721–725
26. Rababa KS, Al-mahasne MM (2011) Effect of roller burnishing on the mechanical behavior and surface quality of o.1 alloy steel. *Res J Appl Sci Eng Technol* 3(3):227–233
27. Rodríguez A, de Lacalle LL, Celaya A, Lamikiz A, Albizuri J (2012) Surface improvement of shafts by the deep ball-burnishing technique. *Surf Coat Technol* 206(11-12):2817–2824
28. Amdouni H, Bouzaiene H, Montagne A, Nasri M, Iost A (2017) Modeling and optimization of a ball-burnished aluminum alloy flat surface with a crossed strategy based on response surface methodology. *Int J Adv Manuf Technol* 88(1):801–814

29. Hamadache H, Bourebia M, Taamallah O, Laouar L (2019) Surface hardening of 36 NiCrMo 6 steel by ball burnishing process. *Mater Res Express* 6(10):106538
30. Jerez-Mesa R, Travieso-Rodríguez JA, Gomez-Gras G, Lluma-Fuentes J (2018) Development, characterization and test of an ultrasonic vibration-assisted ball burnishing tool. *J Mater Process Technol* 257:203–212
31. Amini S, Bagheri A, Teimouri R (2018) Ultrasonic-assisted ball burnishing of aluminum 6061 and AISI 1045 steel. *Mater Manuf Process* 33(11):1250–1259
32. De Lacalle LL, Lamikiz A, Muñoa J, Sánchez J. (2005) Quality improvement of ball-end milled sculptured surfaces by ball burnishing. *Int J Mach Tools Manuf* 45(15):1659–1668
33. Jerez-Mesa R, Landon Y, Travieso-Rodríguez JA, Dessein G, Lluma-Fuentes J, Wagner V (2018) Topological surface integrity modification of AISI 1038 alloy after vibration-assisted ball burnishing. *Surf Coatings Technol* 349:364–377
34. Franzen V, Trompeter M, Brosius A, Tekkaya A (2010) Finishing of thermally sprayed tool coatings for sheet metal forming operations by roller burnishing. *Int J Mater Form* 3(1):147–150
35. Jerez-Mesa R, Fargas G, Roa JJ, Llumà J, Travieso-Rodríguez JA (2021) Superficial effects of ball burnishing on trip steel AISI 301LN sheets. *Metals* 11(1):82
36. El-Taweel T, El-Axir M (2009) Analysis and optimization of the ball burnishing process through the taguchi technique. *Int J Adv Manuf Technol* 41(3-4):301–310
37. Proceso UG-TMP (2010) Use of grey based taguchi method in ball burnishing process for the optimization of surface roughness and microhardness of aa 7075 aluminum alloy. *Mater Tehnologije* 44(3):129–135
38. Teimouri R, Amini S (2019) Analytical modeling of ultrasonic burnishing process: Evaluation of active forces. *Measurement* 131:654–663
39. Standard A (2004) E8-04, Standard test methods for tension testing of metallic materials. *Annu Book ASTM Stand* 3:8
40. ISO D et al Geometrical product specifications (gps)—surface texture: profile method—terms, definitions and surface texture parameters, 4287: 1997/Cor1:1998
41. Avilés R, Albizuri J, Rodríguez A, De Lacalle LL (2013) Influence of low-plasticity ball burnishing on the high-cycle fatigue strength of medium carbon aisi 1045 steel. *Int J Fatigue* 55:230–244
42. Ghafari S, Aziz HA, Isa MH, Zinatizadeh AA (2009) Application of response surface methodology (rsm) to optimize coagulation–flocculation treatment of leachate using poly-aluminum chloride (pac) and alum. *J Hazard Mater* 163(2-3):650–656
43. Wagoner RH, Kim JH, Sung JH (2009) Formability of advanced high strength steels. *Int J Mater Form* 2(1):359–362
44. Ayres R (1983) Evaluating hardening laws at large tensile strains in sheet specimens. *Metall Trans A* 14(11):2269–2275
45. Canales C, Bussetta P, Ponthot J-P (2017) On the numerical simulation of sheet metal blanking process. *Int J Mater Form* 10(1):55–71
46. Yoon JW, Dick R, Barlat F (2011) A new analytical theory for earing generated from anisotropic plasticity. *Int J Plast* 27(8):1165–1184
47. Fargas G, Roa J, Mateo A (2015) Effect of shot peening on metastable austenitic stainless steels. *Mater Sci Eng A* 641:290–296
48. Silva-Álvarez D, Márquez-Herrera A, Saldaña-Robles A, Zapata-Torres M, Mis-Fernández R, Peña-Chapa J, Moreno-Palmerín J, Hernández-Rodríguez E (2020) Improving the surface integrity of the cocrmo alloy by the ball burnishing technique. *J Mater Res Technol* 9(4):7592–7601

**Publisher's note** Springer Nature remains neutral with regard to jurisdictional claims in published maps and institutional affiliations.